

Spin asymmetries for events with high p_T hadrons in DIS and an evaluation of the gluon polarization

*In remembrance of Vernon W. Hughes,
initiator of the SMC experiment and spokesman of the collaboration,
who passed away on March 25, 2003
and to whom this article is dedicated.*

Spin Muon Collaboration (SMC)

B. Adeva²⁰, E. Arik², A. Arvidson^{23,u}, B. Badełek^{23,25}, G. Baum¹, P. Berglund⁸, L. Betev^{13,o}, R. Birsa²², N. de Botton¹⁹, F. Bradamante²², A. Bravar^{11,h}, A. Bressan²², S. Bültmann^{1,v}, E. Burtin¹⁹, D. Crabb²⁴, J. Cranshaw^{18,b}, T. Çuhadar^{2,15}, S. Dalla Torre²², R. van Dantzig¹⁵, B. Derro⁴, A. Deshpande^{26,ih}, S. Dhawan²⁶, C. Dulya^{4,15,c}, S. Eichblatt^{18,d}, D. Fasching^{17,e}, F. Feinstein¹⁹, C. Fernandez^{20,8}, B. Frois¹⁹, A. Gallas²⁰, J.A. Garzon^{20,9}, H. Gilly⁶, M. Giorgi²², E. von Goeler¹⁶, S. Goertz³, G. Gracia^{20,f}, N. de Groot^{15,g}, M. Grosse Perdekamp^{26,jh}, K. Haft¹³, D. von Harrach¹¹, T. Hasegawa^{14,i}, P. Hautle^{5,j}, N. Hayashi^{14,k}, C.A. Heusch^{5,l}, N. Horikawa¹⁴, V.W. Hughes^{26†}, G. Igo⁴, S. Ishimoto^{14,m}, T. Iwata¹⁴, E.M. Kabuß¹¹, A. Karev¹⁰, H.J. Kessler^{6,n}, T.J. Ketel¹⁵, J. Kiryluk^{25,o}, Yu. Kisselev¹⁰, L. Klostermann¹⁵, K. Kowalik²⁵, A. Kotzinian¹⁰, W. Kröger^{5,l}, F. Kunne¹⁹, K. Kurek²⁵, J. Kyyräinen^{1,8}, M. Lamanna^{22,a}, U. Landgraf⁶, J.M. Le Goff¹⁹, F. Lehar¹⁹, A. de Lesquen¹⁹, J. Lichtenstadt²¹, M. Litmaath^{15,a}, A. Magnon¹⁹, G.K. Mallot^{11,a}, F. Marie¹⁹, A. Martin²², J. Martino^{19,y}, T. Matsuda^{14,i}, B. Mayes⁹, J.S. McCarthy²⁴, K. Medved¹⁰, W. Meyer³, D. Miller¹⁷, Y. Miyachi¹⁴, K. Mori¹⁴, J. Moromisato¹⁶, J. Nassalski²⁵, T.O. Niinikoski⁵, J.E.J. Oberski¹⁵, A. Ogawa^{14,h}, C. Ozben^{2,x}, H. Pereira¹⁹, D. Peshekhonov^{10,b}, R. Piegai^{26,p}, L. Pinsky⁹, S. Platchkov¹⁹, M. Plo²⁰, D. Pose¹⁰, H. Postma¹⁵, J. Pretz^{11,w}, G. Rädcl⁵, G. Reicherz³, J. Roberts^q, M. Rodriguez^{23,p}, E. Rondio²⁵, I. Sabo²¹, J. Saborido²⁰, A. Sandacz²⁵, I. Savin¹⁰, P. Schiavon²², E.P. Sichtermann^{15,26,z}, F. Simeoni²², G.I. Smirnov¹⁰, A. Staude¹³, A. Steinmetz¹¹, U. Stiegler⁵, H. Stuhmann⁷, R. Sulej^{25,r}, F. Tessarotto²², D. Thers¹⁹, W. Tłaczala^{25,r}, A. Tripet¹, G. Unel², M. Velasco¹⁷, J. Vogt¹³, R. Voss⁵, C. Whitten⁴, R. Windmolders^{12,w}, R. Willumeit⁷, W. Wiślicki²⁵, A. Witzmann^{6,s}, A.M. Zanetti²², K. Zaremba^{25,r}, J. Zhao^{7,t1}

¹ University of Bielefeld, Physics Department, 33501 Bielefeld, Germany

² Bogaziçi University and Istanbul Technical University, Istanbul, Turkey

³ University of Bochum, Physics Department, 44780 Bochum, Germany

⁴ University of California, Department of Physics, Los Angeles, 90024 CA, USA

⁵ CERN, 1211 Geneva 23, Switzerland

⁶ University of Freiburg, Physics Department, 79104 Freiburg, Germany

⁷ GKSS, 21494 Geesthacht, Germany

⁸ Helsinki University of Technology, Low Temperature Laboratory and Institute of Particle Physics Technology, Espoo, Finland

⁹ University of Houston, Department of Physics, and Institute for Beam Particle Dynamics, Houston, 77204 TX, USA

¹⁰ JINR, Dubna, RU-141980 Dubna, Russia

¹¹ University of Mainz, Institute for Nuclear Physics, 55099 Mainz, Germany

¹² University of Mons, Faculty of Science, 7000 Mons, Belgium

¹³ University of Munich, Physics Department, 80799 Munich, Germany

¹⁴ Nagoya University, CIRSE and Department of Physics, Furo-Cho, Chikusa-Ku, 464 Nagoya, Japan

¹⁵ NIKHEF, Delft University of Technology, FOM and Free University, 1009 AJ Amsterdam, The Netherlands

¹⁶ Northeastern University, Department of Physics, Boston, 02115 MA, USA

¹⁷ Northwestern University, Department of Physics, Evanston, 60208 IL, USA

¹⁸ Rice University, Bonner Laboratory, Houston, 77251-1892 TX, USA

¹⁹ C.E.A. Saclay, DAPNIA, 91191 Gif-sur-Yvette, France

²⁰ University of Santiago, Department of Particle Physics, 15706 Santiago de Compostela, Spain

²¹ Tel Aviv University, School of Physics, 69978 Tel Aviv, Israel

²² INFN Trieste and University of Trieste, Department of Physics, 34127 Trieste, Italy

²³ Uppsala University, Department of Radiation Sciences, 75121 Uppsala, Sweden

²⁴ University of Virginia, Department of Physics, Charlottesville, 22901 VA, USA

²⁵ Soltan Institute for Nuclear Studies and Warsaw University, 00681 Warsaw, Poland

²⁶ Yale University, Department of Physics, New Haven, 06511 CT, USA

We present a measurement of the longitudinal spin cross section asymmetry for deep inelastic muon-nucleon interactions with two high transverse momentum hadrons in the final state. Two methods of event classification are used to increase the contribution of the Photon Gluon Fusion process to above 30%. The most effective one, based on a neural network approach, provides the asymmetries $A_p^{\ell N \rightarrow \ell h h X} = 0.030 \pm 0.057 \pm 0.010$ and $A_d^{\ell N \rightarrow \ell h h X} = 0.070 \pm 0.076 \pm 0.010$. From these values we derive an averaged gluon polarization $\Delta G/G = -0.20 \pm 0.28 \pm 0.10$ at an average fraction of nucleon momentum carried by gluons $\langle \eta \rangle = 0.07$.

PACS numbers: 13.60.Hb, 13.88.+e, 14.70.Dj

I. INTRODUCTION

The Spin Muon Collaboration (SMC) has extensively studied polarized deep inelastic lepton-nucleon scattering using the high energy muon beam at CERN and large polarized hydrogen and deuterium targets. This program was initiated by the observation in a previous CERN experiment (EMC) that only a small fraction of the proton

spin is carried by the spin of the quarks [1]. The SMC results have confirmed this observation for protons and provided the first measurement of the spin structure of deuterons which allowed for the verification of the fundamental Bjorken sum rule [2, 3].

The high energy polarized data from SMC, combined with the high precision data from the SLAC [4] and DESY [5] experiments at lower energy, cover a kinematic range allowing for a QCD analysis of the spin structure function g_1 . Various analyses have been performed at next-to-leading order with different input parameterizations for the polarized parton densities and different choices of the fitted parameters [6, 7]. They provide consistent results for the polarized quark densities but bring little information on the polarized gluon density ΔG . This is an expected feature since g_1 is sensitive to gluons only through its Q^2 evolution and the available g_1 data cover only a narrow range in Q^2 at a given value of x . In particular it is still not possible to test the hypothesis, formulated many years ago, that the gluon spin may account for a sizable fraction of the nucleon spin [8].

A direct measurement of the gluon polarisation is possible via the Photon Gluon Fusion (PGF) process, which is illustrated in Fig.1, together with the two other lowest order diagrams: the virtual photon absorption (leading process "LP") and gluon radiation (QCD Compton scattering "QCD-C"). Since the contribution of the PGF diagram is small, the event selection procedure should be very effective in discriminating the PGF process from other channels. This can be achieved either by selecting events where a charmed particle is produced (e.g. a D meson) or events with hadrons of large transverse momenta (p_T) relative to the virtual photon direction [9, 10]. Both possibilities will be used in the COMPASS experiment presently running at CERN [11].

In this paper we present an evaluation of the gluon polarization, $\Delta G/G$, from the SMC data. We limit the analysis to the DIS region ($Q^2 > 1 \text{ GeV}^2$) and select events with high p_T hadrons. The SMC experimental setup was not optimized for the detection of hadrons produced at large angles, so the precision of the result is obviously limited. This is, however, the first attempt to tag PGF with light quark production in a DIS experiment.

A determination of the gluon polarization from events with high p_T hadrons has been attempted on the ep data from the HERMES experiment [12] at lower incident energy and in a kinematic range where quasi-real photo-

*† Deceased

^a Now at CERN, 1211 Geneva 23, Switzerland

^b Now at Texas Technical University, Lubbock TX 79409-1051, USA

^c Now at CIEMAT, Avda Complutense 22, 28040, Madrid, Spain

^d Now at Fermi National Accelerator Laboratory, Batavia, 60510 Illinois, USA

^e Now at University of Wisconsin, USA

^f Now at NIKHEF, 1009 AJ Amsterdam, The Netherlands

^g Now at Bristol University, Bristol, UK

^h Now at Brookhaven National Laboratory, Upton, 11973 NY, USA

^{ih} Now at Dept. of Physics and Astronomy, SUNY at Stony Brook, Stony Brook, NY 11974, USA

^{jh} Now at Univ. of Illinois at Urbana-Champaign, 405 North Mathews Av. Urbana, Illinois 61801, USA

ⁱ Permanent address: Miyazaki University, Faculty of Engineering, 889-21 Miyazaki-Shi, Japan

^j Permanent address: Paul Scherrer Institut, 5232 Villigen, Switzerland

^k Permanent address: The Institute of Physical and Chemical Research (RIKEN), wako 351-01, Japan

^l Permanent address: University of California, Institute of Particle Physics, Santa Cruz, 95064 CA, USA

^m Permanent address: KEK, Tsukuba-Shi, 305 Ibaraki-Ken, Japan

ⁿ Now at SBC Warburg Dillon Read, CH-4002 Basel, Switzerland

^o Now at University of California, Department of Physics, Los Angeles, 90024 CA, USA

^p Permanent address: University of Buenos Aires, Physics Department, 1428 Buenos Aires, Argentina

^q Permanent address: Rice University, Bonner Laboratory, Houston, TX 77251-1892, USA

^r Permanent address: Warsaw University of Technology, 00-665 Warsaw, Poland

^s Now at F.Hoffmann-La Roche Ltd., CH-4070 Basel, Switzerland

^{t1} Now at Oak Ridge National Laboratory, Oak Ridge, TN 37831-6393, USA

^u Now at The Royal Library, 102 41 Stockholm, Sweden

^v Now at Old Dominion University, Norfolk, VA 23529, USA

^w Now at University of Bonn, 53115, Bonn, Germany

^x Now at University of Illinois at Urbana-Champaign, USA

^y Now at SUBATECH, University of Nantes, UMR IN2P3/CNRS, 44307, Nantes, France

^z Now at Lawrence Berkeley National Laboratory, Berkeley, CA 94720, USA

production is dominant.

II. FORMALISM

Experimentally observed spin-dependent effects are small and have to be determined from the cross section asymmetry defined as the ratio of polarized ($\Delta\sigma$) and unpolarized (σ) cross sections

$$A^{\ell N} = \frac{\Delta\sigma}{2\sigma} = \frac{\sigma^{\uparrow\downarrow} - \sigma^{\uparrow\uparrow}}{\sigma^{\uparrow\downarrow} + \sigma^{\uparrow\uparrow}}, \quad (1)$$

where $\uparrow\downarrow$ and $\uparrow\uparrow$ refer to anti-parallel and parallel configurations of the nucleon and incoming lepton spins. At the parton level the hard scattering cross section consists of three terms corresponding to the LP, QCD-C and PGF processes. According to the factorization theorem σ and $\Delta\sigma$ can be written as convolutions of the parton distributions (F , ΔF), hard-scattering cross sections ($\hat{\sigma}$, $\Delta\hat{\sigma}$) and fragmentation functions D of partons into hadrons:

$$\sigma = F \otimes \hat{\sigma} \otimes D$$

$$\Delta\sigma = \Delta F \otimes \Delta\hat{\sigma} \otimes D. \quad (2)$$

The parton distributions stand for quarks, antiquarks, and gluons. The spin dependent distributions are denoted $\Delta q = q^\uparrow - q^\downarrow$ for quarks, antiquarks and $\Delta G = G^\uparrow - G^\downarrow$ for gluons and the corresponding spin-averaged ones $q = q^\uparrow + q^\downarrow$ and $G = G^\uparrow + G^\downarrow$. Here, the up and down arrows correspond to parallel and anti-parallel configurations of the parton and nucleon spins.

After insertion of the full expression for σ and $\Delta\sigma$ into Eq. (1), the final expression for the cross section asymmetry with production of at least two hadrons with large transverse momenta, $A^{\ell N \rightarrow \ell hhX}$, reads

$$A^{\ell N \rightarrow \ell hhX} = \frac{\Delta q}{q} \langle \hat{a}_{LL} \rangle^{LP} R_{LP} + \langle \hat{a}_{LL} \rangle^{QCD-C} R_{QCD-C} + \frac{\Delta G}{G} \langle \hat{a}_{LL} \rangle^{PGF} R_{PGF}, \quad (3)$$

where $\langle \hat{a}_{LL} \rangle = \langle \Delta\hat{\sigma}/2\hat{\sigma} \rangle$ are the average partonic asymmetries and R the cross section ratios of the different processes shown in Fig. 1, with respect to the total cross section in the selected sample. The asymmetry $A^{\ell N \rightarrow \ell hhX}$ thus permits an evaluation of the gluon polarization if all other elements in Eq. (3) are known. The quark asymmetry $\Delta q/q$ is approximated by the value of A_1 obtained in inclusive measurements. The partonic asymmetries \hat{a}_{LL} are calculated for simulated events and averaged over the selected sample; in the kinematic region covered by the SMC data, they are found to be positive for the first two processes and negative for PGF. The ratios R are taken from the simulated sample to which the same selection criteria are applied as to the data.

The statistical precision of the gluon polarization determined from Eq. (3) depends on the precision of the measured asymmetry $A^{\ell N \rightarrow \ell hhX}$ and on the fraction of PGF events (R_{PGF}) in the final sample. Therefore the aim of the present analysis is to select a large enough sample with a maximal contribution of PGF events.

The description of hadron production in DIS muon data in terms of the three processes of Fig. 1 has been successfully tested in previous experiments [13, 14]. Other processes, such as those involving resolved photons, are expected to have small contributions for Q^2 above 1 GeV² and are not considered here.

III. THE EXPERIMENT

The experimental setup at the CERN muon beam consisted of three major components: a polarized target, a magnetic spectrometer and a muon beam polarimeter. A detailed description of the experiment and of the analysis of the inclusive data can be found in Refs. [3, 15]. The muon beam polarization, P_B , was determined from the spin asymmetries measured in polarized muon-electron scattering and from the energy spectrum of positrons from muon decays and was found to be -0.795 ± 0.019 for an average beam energy of 187.4 GeV [16]. The target consisted of two cells filled with butanol, deuterated butanol or ammonia [17]. The two cells were polarized in opposite directions by dynamic nuclear polarization. The average target polarizations, P_T , were approximately 0.90 for protons and 0.50 for deuterons, with a relative error $\Delta P_T/P_T$ of 3-5%. The polarization was reversed five times a day.

The counting rate asymmetry, A^{exp} , is determined from the number of events counted in upstream and downstream target cells before and after polarization reversal. This is done by solving the resulting second order equation, as described in [18].

The cross-section asymmetry, $A^{\ell N \rightarrow \ell hhX}$, is related to A^{exp} by:

$$A^{\ell N \rightarrow \ell hhX} = \frac{1}{P_B P_T f} A^{exp}, \quad (4)$$

where f is the effective dilution factor, which takes into account the dilution of spin asymmetries by the presence of unpolarizable nuclei in the target and also by radiative effects on the nucleon. The effect of unpolarizable materials can be expressed in terms of the numbers n_A of nuclei with mass number A and the corresponding total spin-independent cross sections σ_A^{tot} . The radiative effects on the nucleon [15, 19] are taken into account through the ratio of one photon exchange to total cross-sections $\rho = \sigma_{p,d}^{1\gamma}/\sigma_{p,d}^{tot}$. The evaluation of the effective dilution factor for inclusive events and for events with observed hadrons is described in Ref. [3]. Polarized radiative corrections are applied to the asymmetries as described in Refs. [15, 20]. In this analysis polarized radiative cor-

rections and dilution due to radiative effects are reduced because processes without hadrons are excluded.

IV. SAMPLE SELECTION

The total sample of data collected by the SMC experiment during the years 1993-1996 with muon beam of $E=190$ GeV and longitudinally polarized target was used for the analysis. It consists of samples of similar size taken on polarized protons and deuterons.

The standard cuts on inclusive kinematic variables [3], $\nu = E - E' > 15$ GeV and $E' > 19$ GeV were imposed to reject events with poor kinematic resolution and muons from hadron decay, respectively. The cut $y = \nu/E < 0.9$ removes a region where the uncertainty due to radiative corrections becomes large. Two other cuts were applied in close relation to the formalism used in the analysis: a cut $Q^2 > 1$ GeV² rejects the region dominated by non-perturbative effects and allows to interpret the results in terms of partons. A cut $y > 0.4$ removes events which carry little spin information due to a small virtual photon polarization. In addition, cuts on the muon scattering angle were applied in order to match the angular acceptance of the hardware triggers.

In the leading process (LP) most hadrons have small p_T as only the intrinsic k_T of quarks in the nucleon [21] and the fragmentation mechanism contribute to it. A different situation occurs for QCD-C and PGF, where hadrons mainly acquire transverse momentum from primarily produced partons. For this reason, the requirement of two observed hadrons with large transverse momenta enhances the contribution of the PGF and QCD-C processes in the selected sample.

In the present analysis, the events of interest include a reconstructed beam muon, a scattered muon, and at least two charged hadrons. They represent about 20% of the total number of events with reconstructed beam and scattered muons, used for inclusive studies. Hadron tracks were accepted if they could be associated to the primary interaction point, i.e. the vertex, defined by the beam and scattered muons. The same association criteria as in the SMC analysis of Ref. [3] were applied. In order to suppress the contribution from the target fragmentation region, cuts on the reduced longitudinal momentum of the hadron, $x_F > 0.1$, and on the hadron fractional energy, $z = E_h/\nu > 0.1$, were applied.

The further requirement of two hadrons with $p_T > 0.7$ GeV selects about 5% of the events passing all previous cuts. The electron contamination to this sample is expected to be negligible because electrons are generally produced at low p_T . This is confirmed by the ratio of the energy deposited in the electromagnetic part of the calorimeter to the total deposited energy, which does not show any peak at 1.0 for tracks with $p_T > 0.5$ GeV. After all selections the total number of remaining events amounts to about 80k for the proton and 70k for the deuteron sample.

V. MONTE CARLO SIMULATION

A. Conditions for MC generation

The interactions were simulated using the LEPTO 6.5 generator [22] with a leading order parameterization of the unpolarized parton distributions [23]. The spin dependent effects were calculated using POLDIS [24] with a consistent set of polarized parton distributions [25]. The kinematic limits of the MC generation were defined so as to cover the full kinematic region of the data. Default values were used for most of the steering parameters of the LEPTO generator. Below we discuss only the modified conditions and parameters.

The matrix elements of first order QCD processes exhibit collinear divergences in the cross channel and different schemes are used to avoid such singularities. The so-called $z\hat{s}$ scheme, which allows for lower values of the γ^* -parton center of mass energy $\sqrt{\hat{s}}$, was used in the simulation with modified cut-off parameters. The effect of the cut-off values on any observable distribution for events with high p_T hadrons is only marginal.

The description of interactions requires the choice of two scales: a factorization scale, which appears in the parton densities, and a renormalization scale which appears in expressions depending on the strong coupling constant α_s . Here the usual choice of Q^2 was made in both cases. In these conditions, after kinematic cuts on event variables only, the generated sample contains 8% PGF events.

In order to describe the data, it was found necessary to change the values of two fragmentation parameters in JETSET [26]. The function $f(z) = z^{-1}(1-z)^a e^{-bm_T^2/z}$, where $m_T^2 = m^2 + p_T^2$ and m is the mass of the quark, expresses the probability that a fraction z of the available energy will be carried away by a newly created hadron. The parameters (a , b) were modified from their default values (0.3, 0.58) to (0.5, 0.1), a change making the fragmentation softer. This modification was inspired by a similar study done by the HERMES experiment [27, 28] and seems to work also in the present case, with smaller deviations from the default values. However, we are looking here at a particular sample and have no possibility to check if the Monte Carlo sample generated with these modifications would correctly describe the full data. The uncertainty connected with these modifications has been estimated and included in the systematic error.

B. Simulation of experimental conditions

The scattered muon track of each simulated event was followed through the magnet aperture. Trigger conditions were checked and prescaling factors applied in order to reproduce the relative trigger rates in the simulated sample. Kinematic smearing was applied to muon and hadron tracks and geometric smearing to the vertex position. In addition, the loss of tracks due to chamber

inefficiencies was taken into account by applying detector plane efficiencies to the simulated events and by removing the tracks which did not fulfill the minimal requirements for reconstruction.

Secondary interactions of hadrons have to be taken into account to reproduce the distribution of interaction vertices along the target axis. Hadrons were rejected from the sample according to the probability of re-interaction in the polarized target material. As an example, Fig. 2 shows the agreement obtained for the vertex position along the beam axis in one of the proton data sets.

The simulation was performed for each year of data taking separately. To get a good description of the kinematic variables it was required to use specific beam parameters for every year, including small changes in angles, and to take into account the exact target position.

C. Comparison of simulations and data

The distributions of kinematic variables as well as the particle distributions in detectors were checked with identical selection criteria applied to data and MC. For the simulated events the cuts were applied to the smeared variables. The distributions for data and MC were normalized to the same number of events. The distributions of x and Q^2 for interactions on protons are presented in Fig. 3. The obtained agreement is at the level of 10-25% for all kinematic event variables. The level of agreement for deuterons is very similar [29].

The same comparisons were done for hadron variables. For simulations performed with the unmodified fragmentation function clear discrepancies are observed for the hadron production angle θ and the longitudinal momentum p_L , while satisfactory agreement is obtained for p_T , except at the highest values. The observed differences at the highest values of p_T can be explained by the approximate description of the non-Gaussian tails of the distributions used for smearing and by the effects of real photon radiation, which are not taken into account in the present analysis. It was checked that the discrepancy for the θ angle could not be removed by using different smearing parameterizations or even by an artificial increase of smearing. Agreement between data and simulation could only be achieved by applying a cut on the hadron production angle $\theta > 0.02$ rad. This cut, however, removes about 25% of the selected sample and cannot be justified since there is no reason why the simulation should not describe the hadrons produced at low θ . Therefore modified simulation conditions providing a better description of the data were searched for.

When the modifications of the fragmentation function parameters are applied (cf. Section V.A), the agreement becomes satisfactory over a wide range of θ and p_L . The comparison of the p_L and θ distributions is shown in Fig. 4 for the hadron with highest p_T . The second hadron is also well described by the MC [29]. We concluded that the parameters of the longitudinal frag-

mentation function $f(z)$ have to be modified in order to obtain a good description of the data over the full range of hadron production angle θ . Since it is difficult to check if the modified set of parameters correctly describes the semi-inclusive hadron distributions, the analysis has been performed in parallel with modified fragmentation as well as with the standard fragmentation and an additional cut on $\theta > 0.02$ rad.

VI. SELECTION OF THE PGF PROCESS

In order to compare the merits of various selections of PGF events, we will use the *efficiency* ϵ , which is the ratio of the number of PGF events accepted by the selection criteria to the total number of PGF events, and the *purity* R_{PGF} (Eq.3), which is the ratio of the number of selected PGF events to the total number of selected events. The optimal selection is obviously the one providing the highest values of ϵ and R_{PGF} but, in general, an increase of the former will result in a decrease of the latter.

The purity is 0.11 for the full sample of events with at least 2 charged hadrons. The additional requirement of two hadrons with $p_T > 0.7$ GeV defines our reference sample for which $R_{PGF} = 0.24$ and, by definition, $\epsilon = 1$.

The effects of cuts were studied for the following variables: p_{T1} , the sum $p_{T1}^2 + p_{T2}^2$, hadron charges (same or opposite sign), the azimuthal angle ϕ between the momenta of the two hadrons with respect to the virtual photon direction, and the invariant mass of the two hadrons (see also Ref. [30]). It was found that the selection on $\sum p_T^2$ is optimal for enhancing the PGF purity and that further requirements on the hadron charges do not bring any significant improvement. Fig. 5 shows the variation of R_{PGF} with ϵ when the cut on $\sum p_T^2$ is varied up to 4 GeV². It is seen that the purity increases only very slowly when the cut is made more restrictive while the efficiency drops very rapidly. This can be understood by the fact that one of the background processes (QCD-C) has a similar dependence on the $\sum p_T^2$ cut as PGF. The approximation made in Eq. (3) by the use of A_1 for the asymmetry on quarks is only valid if the fraction of PGF events in the selected sample is much higher than in the inclusive one, i.e. close to the maximum value of 0.33. The efficiency also needs to be sufficiently high to allow a meaningful analysis. As a compromise, we have fixed the cut at 2.5 GeV², which corresponds to $\epsilon = 0.30$ and $R_{PGF} = 0.31$.

The combination of several variables into a single parameter has also been investigated in a classification procedure based on a neural network [29, 31]. We considered the variables which characterize the DIS event (x , Q^2 , y , and the multiplicity of tracks) and those which describe the two selected hadrons with highest p_T (transverse and longitudinal hadron momenta, charges of the hadrons, energy fraction of the hadrons, and the azimuthal angle ϕ). The classification procedure was trained on a

Monte Carlo sample where the actual process is known for each event. As a result, the procedure provides a single value, called "NN response", within the range (0,1). High values of this response correspond to events which, according to the classification algorithm, are more likely to be PGF than background processes. A threshold on the network response can thus be used to select a PGF enriched sample.

The variation of R_{PGF} vs. ϵ for various choices of the NN response threshold is also shown in Fig. 5. It is observed that at equal efficiency the NN approach always provides samples with higher purity than the selection based on $\sum p_T^2$. For further analysis, a threshold of 0.26 was chosen, which corresponds to $R_{PGF} = 0.33$ and $\epsilon = 0.56$. A similar purity is obtained with the $\sum p_T^2$ cut at 2.5 GeV^2 but with an efficiency of 30%. Therefore a better statistical precision on the measured asymmetry will be obtained with the neural network method. Alternatively, a higher NN threshold corresponding to a PGF efficiency of 30% would yield a sample where the purity is about 37%, i.e. 6% higher than the value obtained with the $\sum p_T^2$ cut. The comparison of the two selected samples shows that the NN procedure selects a large fraction of events with $\sum p_T^2 > 2.5 \text{ GeV}^2$ but also covers the lower range of $\sum p_T^2$. It was also checked that the distributions of NN responses are compatible for data and Monte-Carlo events.

VII. SPIN ASYMMETRIES $A^{\ell N \rightarrow \ell hh X}$

The SMC data taken from 1993 to 1996 were split into periods of data taking, corresponding to about 15 days each. The asymmetry for a given year is the weighted average of the asymmetries calculated for each period of data taking. Splitting the data into smaller subsamples gives identical results within the expected statistical fluctuations. The distribution of the vertex position along the beam axis, as presented in Fig. 2, shows that the ratio of acceptances for the upstream to downstream target cells is about 0.7. The method used for asymmetry calculation, described in [18], is suited for such an acceptance difference.

The asymmetry calculations were done for the entire sample which has a purity $R_{PGF} = 0.24$ and for the two selection methods with enhanced R_{PGF} ($\sum p_T^2 > 2.5 \text{ GeV}^2$ and NN response > 0.26). The results given in Fig. 6 and Table I show that the asymmetries do not change significantly with the selection. Also the asymmetries obtained for proton and deuteron are compatible within errors. The statistical error is larger for the selection based on $\sum p_T^2$ because a smaller fraction of events is selected (28 % vs. 42 %).

The errors of the measured $A^{\ell N \rightarrow \ell hh X}$ asymmetry for the selected samples are dominated by statistics. The contributions to the systematic uncertainty on $A^{\ell N \rightarrow \ell hh X}$ are detailed in Table II for the two selections with enhanced R_{PGF} . The most significant ones

come from the false asymmetries, the fraction of radiative processes (ρ) and the polarized radiative corrections. For the false asymmetries an upper limit from the time variation of the acceptance was taken under the assumption that the reconstruction for each of the three tracks (scattered muon and two hadrons) is affected independently. The method used for estimating these effects is described in Ref.[30]. The radiative corrections are small due to the limited phase space for real photon emission in events where a significant fraction of the available energy is taken by the two hadrons with large p_T . The uncertainties in ρ and polarized radiative corrections were taken equal to the full size of the inelastic contribution. The effect of real photon radiation on the event kinematics and, in particular, on the value of p_T itself has not been taken into account in view of the limited precision of the present analysis.

VIII. DETERMINATION OF THE GLUON POLARIZATION

The gluon polarization is evaluated from Eq. (3) using the measured $A^{\ell N \rightarrow \ell hh X}$ asymmetry, obtained for the samples with enhanced R_{PGF} , quoted in Table 1. In view of the strong dependence of the resulting gluon polarization on the information obtained from the Monte Carlo, special attention was given to the agreement of data and simulated events (Figs.2-4).

The asymmetry $A_1(x)$ for each event is taken from a fit to all experimental data and averaged for the full proton and deuteron samples. The partonic asymmetries \hat{a}_{LL} for each sub-process are calculated for each Monte-Carlo event and averaged. Their averaged values for LP and QCD-C are very similar for the two selections namely, $\langle \hat{a}_{LL} \rangle^{LP} = 0.8$ and $\langle \hat{a}_{LL} \rangle^{QCD-C} = 0.6$. The values for PGF are $\langle \hat{a}_{LL} \rangle^{PGF} = -0.44$ and -0.49 for the $\sum p_T^2$ cut and the NN selection, respectively. After selection on $\sum p_T^2$ the final proton sample consists of 26% LP, 43% QCD-C and 31% PGF, while for the neural network the fractions are $R_{LP} = 38\%$, $R_{QCD-C} = 29\%$ and $R_{PGF} = 33\%$. The contributions of different processes for the proton and deuteron samples differ by less than 2%.

The gluon polarization is determined for the kinematic region covered by the selected sample and corresponds to a given fraction of nucleon momentum carried by gluons η :

$$\eta = x \left(\frac{\hat{s}}{Q^2} + 1 \right). \quad (5)$$

This quantity is known for simulated events but cannot be directly determined from the data. Nevertheless, \hat{s} can be approximately calculated from the virtual photon energy in the laboratory system and from the angles (θ_1 , θ_2) defined by the directions of the two hadrons with respect to the virtual photon:

$$\hat{s} \approx \nu^2 \text{tg}\theta_1 \text{tg}\theta_2. \quad (6)$$

To check the validity of this approximation in our kinematic conditions, we have compared the generated η and the one calculated from the above equation for selected PGF events. The calculated values are on average 25% higher than the generated ones. The averaged value of the generated η for the selected PGF events in the Monte Carlo is used as the reference value for the result on $\Delta G/G$. We have also checked the average values of η calculated for all simulated events and obtained the values 0.15 for the cut $\sum p_T^2 > 2.5 \text{ GeV}^2$ and 0.10 for the NN response > 0.26 . For both selection methods the values of η calculated for all simulated events and for data are very close. The results on the gluon polarization and the values of $\langle \eta \rangle$ are presented in Table III.

In addition to the systematic errors on the measured asymmetry discussed in Section 7 and given in Table II, the asymmetry A_1 , the fractions R , and the partonic asymmetries $\langle \hat{a}_{LL} \rangle$ contribute to the systematic error on $\Delta G/G$. The contribution due to the asymmetry A_1 is determined from the uncertainty on A_1 at the averaged value of x and thus from the errors on the fit parameters. The value of A_1 at the average x agrees with the average A_1 calculated from the fit for each event to within 0.001.

The dominant contributions to the systematic error are due to the uncertainties on the values of R and $\langle \hat{a}_{LL} \rangle$. They are estimated by comparing the results obtained from Monte Carlo simulations with different parameters. For this purpose, a sample of LEPTO events was generated with the same kinematic and hadron selections but with modified renormalization and factorization scales, cut-offs and fragmentation function parameters. Scales of $Q^2/2$ and $2 Q^2$ were used for comparison and provide an estimate of the stability of the leading order approximation used here. Results with standard and modified parameters (see Section 5.1) in the fragmentation function were compared. Since only the simulations which reproduce the data should be considered, a cut on the hadron angle θ was applied, as explained in Section 5.3. The value of the gluon polarization calculated with this new Monte Carlo sample was compared to the one obtained under the conditions described in Section 5.1. This procedure was repeated several times with slightly different cuts and with different neural network thresholds. For the neural network the procedure is complicated by the fact that any change in the simulation procedure leads to a different selection on the data. To avoid the fluctuation of the gluon polarization due to variation of the measured asymmetry, the value of this asymmetry was artificially frozen when comparing results for different MC samples. The individual contributions to the systematic error are given, for both selection methods, in Table IV. It was checked that the effect of combined modifications in the Monte Carlo is smaller than the sum of the individual uncertainties. The maximal variation of R_{PGF} and $\langle \hat{a}_{LL} \rangle$ was found to be 20% and 4% respectively.

As discussed before, the neural network selection provides a more accurate result than the selection based on Σp_T^2 cuts. However, the statistical error is too large to

draw definitive conclusions on the contribution of ΔG to the nucleon spin. The systematic uncertainty is small compared to the statistical error. The demand of a good agreement of the simulation with the data sets an important limitation on the estimated systematic uncertainties. For this reason, an increase in statistical precision is expected also to lead to further improved systematic uncertainty estimates.

Averaging the results for proton and deuteron obtained with the neural network classification we obtain $\Delta G/G = -0.20 \pm 0.28 \pm 0.10$.

IX. CONCLUSIONS

We have evaluated for the first time the gluon polarization from the spin asymmetries measured in lepton-nucleon DIS events with $Q^2 > 1 \text{ GeV}^2$ including two hadrons with large transverse momentum in the final state. The analysis is performed at leading order in QCD and based on the comparison of selected data samples with simulated events provided by the LEPTO generator. The partonic asymmetry \hat{a}_{LL} is mostly negative for the photon-gluon fusion process while it is positive for the two competing processes, leading process and gluon radiation. The relative contribution of photon-gluon fusion is enhanced to about 30% by applying a cut on $\Sigma p_T^2 > 2.5 \text{ GeV}^2$ or by using a neural network classification.

The average gluon polarization obtained for the SMC data is close to zero with a large statistical error (~ 0.30). The accuracy is limited by the reduction to less than 1% of the DIS sample by the hadron selection requirements. It is thus expected to be improved by higher counting rates and larger hadron acceptance in ongoing and future experiments.

ACKNOWLEDGMENT

This work was supported by Bundesministerium für Bildung, Wissenschaft, Forschung und Technologie, partially supported by TUBITAK and the Center for Turkish-Balkan Physics Research and Application (Bogziçi University), supported by the U.S. Department of Energy, the U.S. National Science Foundation, Monbusho Grant-in-Aid for Science Research (International Scientific Research Program and Specially Promoted Research), the National Science Foundation (NWO) of the Netherlands, the Commissariat à l'Énergie Atomique, Comision Interministerial de Ciencia y Tecnologia and Xunta de Galicia, the Israel Science Foundation, and Polish State Committee for Scientific Research (KBN) SPUB no. 134/E-365/SPUB-M/CERN/P-03/DZ299/2000 and 621/E-78/SPB/CERN/P-03/DWM 576/2003-2006 and Grant No. 2/P03B/10725.

-
- [1] EMC, J. Ashman *et al.*, Nucl. Phys. B **328**, 1 (1989); Phys.Lett.B **206**, 364 (1988).
- [2] SMC, B. Adeva *et al.*, Phys. Lett. B **302**, 533 (1993).
- [3] SMC, B. Adeva *et al.*, Phys. Rev. **D58**, 112001 (1998).
- [4] E142, P.L. Anthony *et al.*, Phys. Rev. D **54**, 6620 (1996); E143, K. Abe *et al.*, Phys. Rev. D **58**, 112003 (1998); E154, K. Abe *et al.*, Phys. Rev. Lett. **79**, 26 (1997); E155, P. L. Anthony *et al.* Phys. Lett. B **458**, 529 (1999).
- [5] HERMES, A. Airapetian *et al.*, Phys. Lett. B **442**, 484 (1998).
- [6] SMC, B. Adeva *et al.*, Phys. Rev. D **58**, 112002 (1998); E155, P. L. Anthony *et al.*, Phys. Lett. B **493**, 19 (2000).
- [7] G. Altarelli, R. D. Ball, S. Forte and G. Ridolfi, Nucl. Phys. B **496**, 337 (1997); E. Leader, A. V. Sidorov and D. B. Stamenov, Eur. Phys. J. C **23**, 479 (2002); Y. Goto *et al.*, Phys. Rev. D **62** (2000) 034017; M. Glück, E. Reya, M. Stratmann and W. Vogelsang, Phys. Rev. D **63**, 094005 (2001); J. Blümlein and H. Bottcher, Nucl. Phys. B **636**, 225 (2002); C. Bourrely, J. Soffer and F. Buccella, Eur. Phys. J. C **23**, 487 (2002).
- [8] A.V. Efremov and O.V. Teryaev, JINR Report E2-88-287, Dubna (1988); G. Altarelli and G.G. Ross, Phys. Lett. B **212**, 391 (1988).
- [9] R.D. Carlitz, J.C. Collins and A.H. Mueller, Phys. Lett. B **214**, 229 (1988).
- [10] A. Bravar, D. von Harrach and A. Kotzinian, Phys. Lett. B **421**, 349 (1998).
- [11] COMPASS, G. Baum *et al.*, 'COMPASS: A Proposal for a Common Muon and Proton Apparatus for Structure and Spectroscopy', CERN-SPSLC-96-14.
- [12] HERMES, A. Airapetian *et al.*, Phys. Rev. Lett. **84**, 2584 (2000).
- [13] EMC, M. Arneodo *et al.*, Phys. Lett. B **149**, 415 (1984); Z. Phys. C **36**, 527 (1987).
- [14] E665, M.R. Adams *et al.*, Phys. Rev. D **48**, 5051 (1993); Phys.Rev.Lett.**72**, 466 (1994).
- [15] SMC, D. Adams *et al.*, Phys. Rev. D **56**, 5330 (1997).
- [16] SMC, B. Adeva *et al.*, Nucl. Instr. and Meth. A **443**, 1 (2000).
- [17] SMC, B. Adeva *et al.*, Nucl. Instr. and Meth. A **437**, 23 (1999).
- [18] L. Klosterman, Ph.D. thesis, Delft University of Technology, Delft (1995).
- [19] A.A. Akhundov *et al.*, Fortsch. Phys. **44**, 373 (1996); Sov. J. Nucl. Phys. **26**, 660 (1977); *ibid.* **44**. 988 (1986); D. Bardin and N. Shumeiko, Sov. J. Nucl. Phys. **29**, 499 (1979).
- [20] T.V. Kukhto and N.M. Shumeiko, Nucl. Phys. B **219**, 412 (1983).
- [21] A. König, Z. Phys. C **18**, 63 (1983).
- [22] G. Ingelman, A. Edin and J. Rathsman, Comput. Phys. Commun. **101**, 108 (1997).
- [23] M. Glück, E. Reya and A. Vogt, Z. Phys. C **67**, 433 (1995).
- [24] A. Bravar, K. Kurek and R. Windmolders, Comput. Phys. Commun. **105**, 42 (1997).
- [25] T. Gehrmann and W.J. Stirling, Phys. Rev. D **53**, 6100 (1996).
- [26] T. Sjöstrand *et al.*, Comput. Phys. Commun. **135**, 238 (2001).
- [27] N.C.R. Makins, HERMES, private communication (2002).
- [28] P. Geiger, Ph.D. Thesis, University of Heidelberg (1998).
- [29] K. Kowalik, Ph.D. Thesis, Institute for Nuclear Studies, Warsaw (2004).
- [30] H. Gilly, Ph.D. Thesis, University of Freiburg (2000).
- [31] K. Kowalik *et al.*, Acta Physica Polonica B **32**, 2929 (2001).

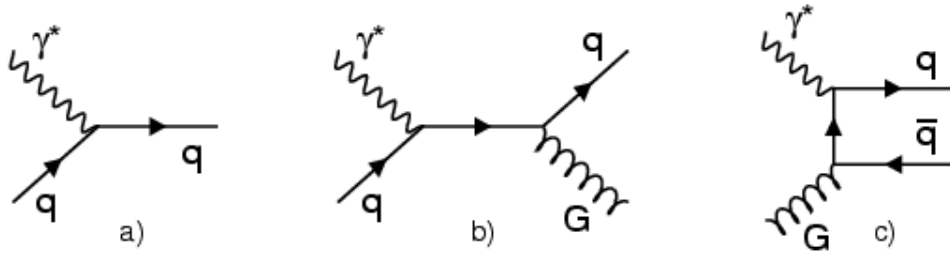


FIG. 1: Lowest order diagrams for DIS γ^* absorption: a) leading process (LP), b) gluon radiation (QCD-C), c) photon-gluon fusion (PGF).

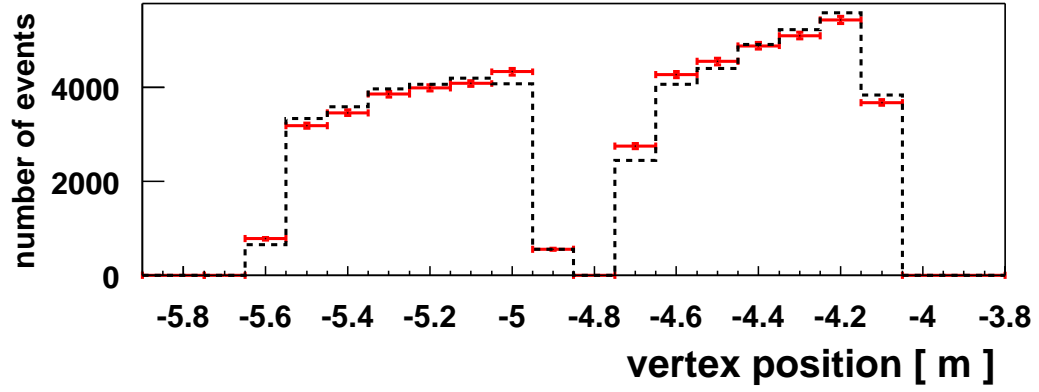


FIG. 2: Distribution of vertices along the beam axis. Points correspond to the proton data from 1993 and the histogram to the corresponding MC simulation.

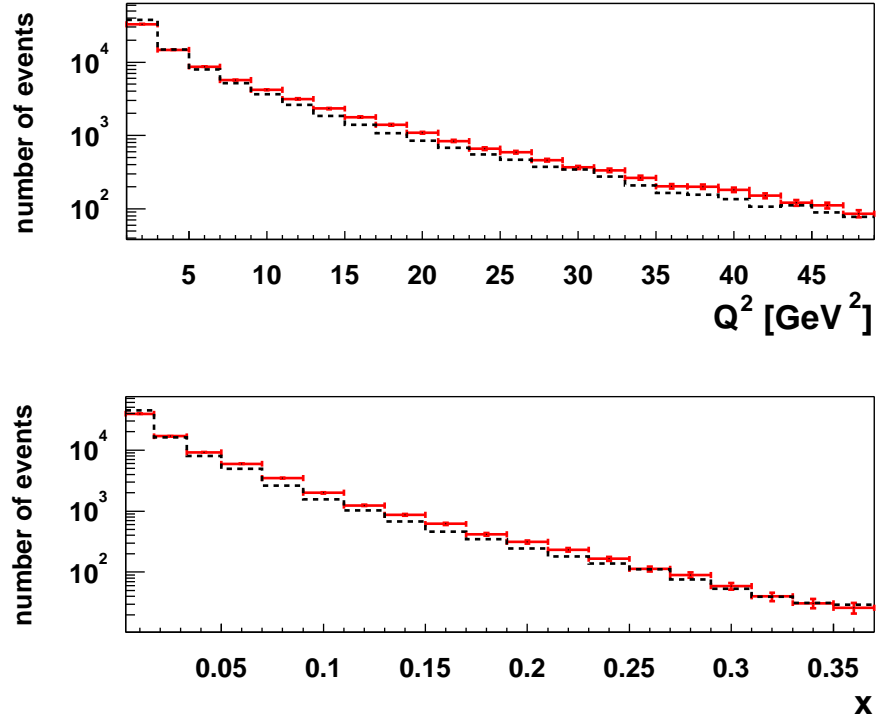


FIG. 3: The x and Q^2 distributions for the proton case: points correspond to the data and histograms to the Monte Carlo simulation.

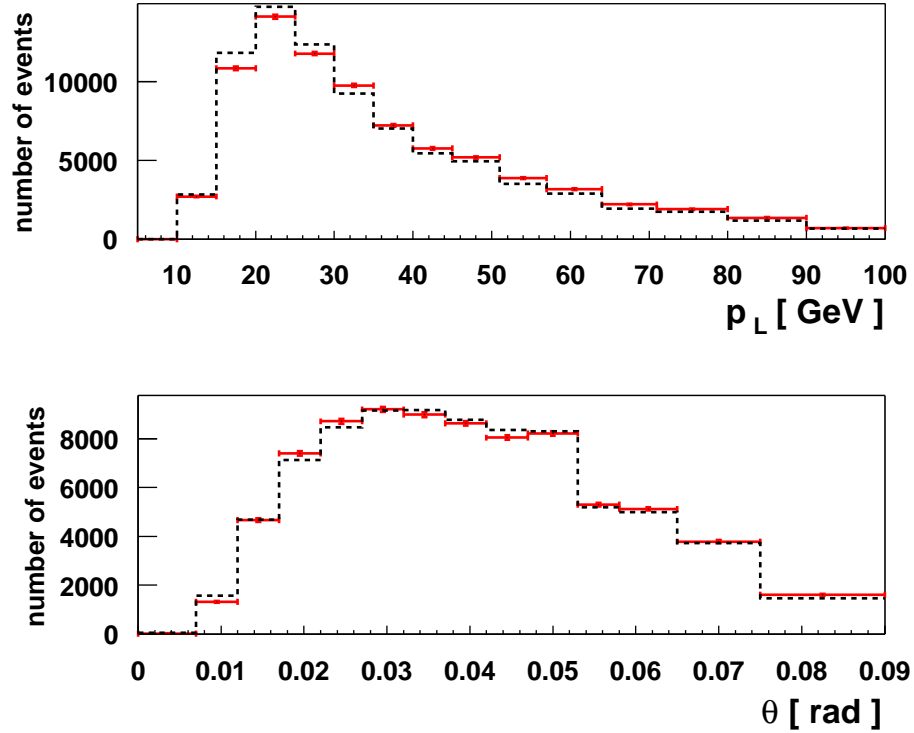


FIG. 4: Distributions of longitudinal momentum and scattering angle for the hadron with the highest p_T . Points correspond to the proton data collected in 1993, histograms to the Monte Carlo simulations with the modified fragmentation function.

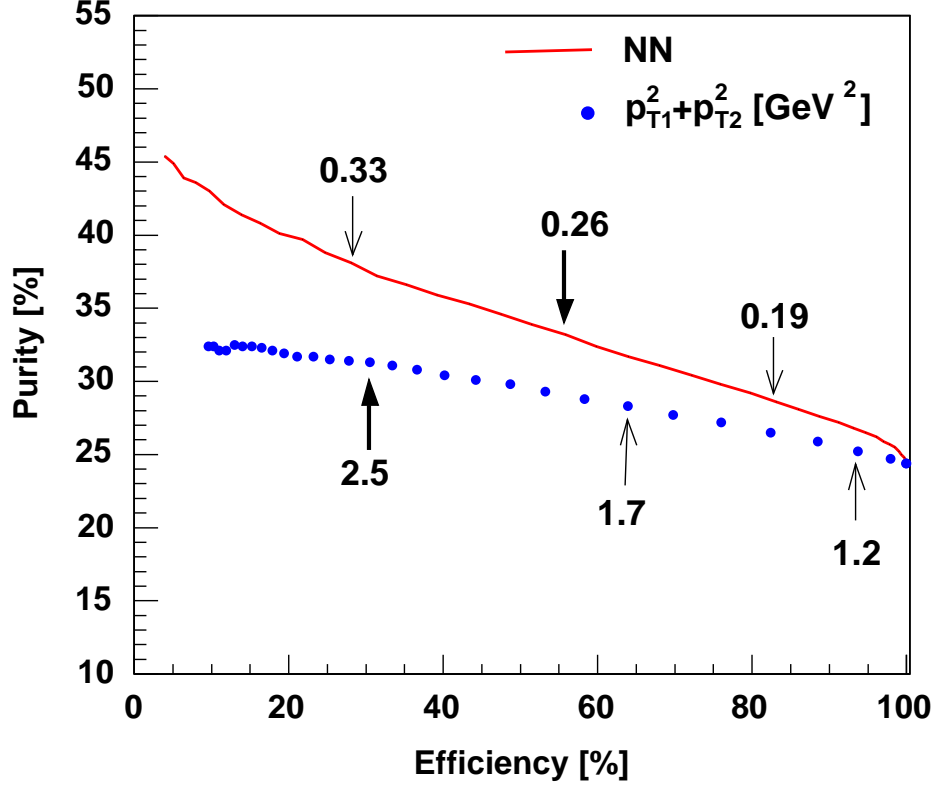


FIG. 5: Comparison of purity and efficiency for the selection methods based on the cut on $\sum p_T^2$ and the NN response. Simulations correspond to the proton sample.

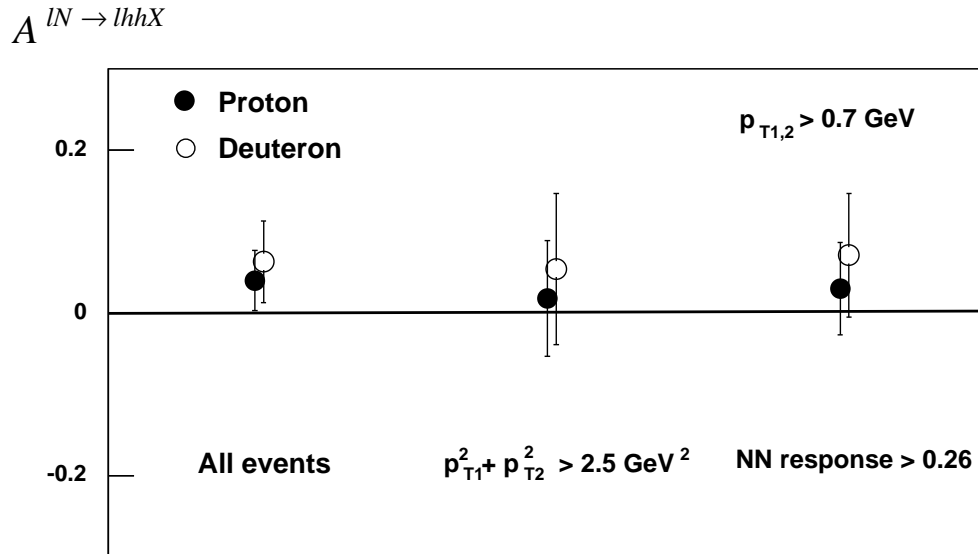


FIG. 6: Measured asymmetry $A^{\ell N \rightarrow \ell h h X}$, for proton and deuteron, for events with $p_{T1,2} > 0.7$ GeV cut and after additional selections on $\sum p_T^2$ and neural network threshold to increase the purity.

TABLE I: Measured cross-section asymmetries $A^{\ell N \rightarrow \ell h h X}$ for proton and deuteron events with $p_{T1,2} > 0.7$ GeV and in the samples selected with the $\sum p_T^2$ cut and with the neural network response threshold, each given with statistical and systematic errors.

Selection	$A_p^{\ell N \rightarrow \ell h h X}$	$A_d^{\ell N \rightarrow \ell h h X}$
All	$0.041 \pm 0.037 \pm 0.011$	$0.063 \pm 0.050 \pm 0.011$
$\sum p_T^2 > 2.5 \text{ GeV}^2$	$0.018 \pm 0.071 \pm 0.010$	$0.054 \pm 0.093 \pm 0.008$
NN response > 0.26	$0.030 \pm 0.057 \pm 0.010$	$0.070 \pm 0.076 \pm 0.010$

TABLE II: The contributions to the systematic error of $A^{\ell N \rightarrow \ell h h X}$ with the $\sum p_T^2 > 2.5 \text{ GeV}^2$ cut and with the neural network response > 0.26 for SMC proton and deuteron data. The first and last contributions are additive; the others are proportional to the asymmetry.

Contributions to the systematic error on $A^{\ell N \rightarrow \ell h h X}$	proton data		deuteron data	
	$\sum p_T^2$	NN	$\sum p_T^2$	NN
False asymmetries	0.0049	0.0049	0.0044	0.0044
Target polarization	0.0005	0.0008	0.0016	0.0023
Beam polarization	0.0007	0.0011	0.0021	0.0029
Dilution factor				
Target composition	0.0003	0.0001	0.0002	0.0001
ρ factor	0.0018	0.0030	0.0054	0.0076
Polarized rad. corr.	0.0083	0.0083	0.0020	0.0020
Total systematic error	0.0098	0.0102	0.0077	0.0097

TABLE III: Gluon polarization for proton and deuteron for the $\sum p_T^2$ cut and the neural network selection.

Selection	$\left(\frac{\Delta G}{G}\right)_p$	$\left(\frac{\Delta G}{G}\right)_d$	$\langle \eta \rangle$
$\sum p_T^2 > 2.5 \text{ GeV}^2$	$0.11 \pm 0.51 \pm 0.12$	$-0.37 \pm 0.66 \pm 0.12$	0.09
NN response > 0.26	$-0.06 \pm 0.35 \pm 0.10$	$-0.47 \pm 0.49 \pm 0.10$	0.07

TABLE IV: Contributions to the systematic error on gluon polarization for two methods of event selection.

Source of the uncertainty	Σp_T^2	NN
systematic error on $A^{\ell N \rightarrow \ell h h X}$	0.072(p) 0.057(d)	0.061(p) 0.063(d)
precision of A_1 fit	0.042(p) 0.042(d)	0.026(p) 0.028(d)
scale change from $Q^2/2$ to $2 Q^2$	0.008	0.010
fragmentation paramr.	0.036	0.034
cut-offs in matrix elem.	0.015	0.008